Open access • Posted Content • DOI:10.1101/2021.08.08.455564

Mitonuclear co-introgression opposes genetic differentiation between phenotypically divergent songbirds — Source link

Ellen Nikelski, A. S. Rubtsov, Darren E. Irwin

Institutions: University of Toronto, University of British Columbia

Published on: 08 Aug 2021 - bioRxiv (Cold Spring Harbor Laboratory)

Topics: Introgression, Mitochondrial DNA and Nuclear gene

Mitonuclear co-introgression opposes genetic differentiation between phenotypically divergent songbirds

Ellen Nikelski[1, *], Alexander S. Rubtsov[2], and Darren Irwin[1]

[1] Department of Zoology, and Biodiversity Research Centre, 6270 University Blvd., University of British Columbia, Vancouver, BC, Canada

[2] State Darwin Museum, Moscow, Russia

[*] Present address: Department of Ecology and Evolutionary Biology, University of Toronto, Toronto, ON, Canada

Running Title:

Co-introgression opposes differentiation

Corresponding Author:

Ellen Nikelski, Department of Ecology and Evolutionary Biology, University of Toronto, Toronto, ON, Canada. Email: ellen.nikelski@mail.utoronto.ca

Keywords:

mitonuclear co-introgression, mtDNA, mitonuclear gene, genetic differentiation, chromosome Z, Aves

Abstract

Comparisons of genomic variation among closely related species often show more differentiation in mitochondrial DNA (mtDNA) and sex chromosomes than in autosomes, a pattern expected due to the relative effective population sizes of these genomic components. Differential introgression can cause some species pairs to deviate dramatically from this pattern. The yellowhammer (*Emberiza citrinella*) and the pine bunting (*E. leucocephalos*) are hybridizing avian sister species that differ greatly in appearance but show no mtDNA differentiation. This discordance might be explained by mtDNA introgression—a process that can select for co-introgression at nuclear genes with mitochondrial functions (mitonuclear genes). We investigated genome-wide nuclear differentiation between yellowhammers and pine buntings and compared it to what was seen previously in the mitochondrial genome. We found clear nuclear differentiation that was highly heterogeneous across the genome, with a particularly wide differentiation peak on the sex chromosome Z. We further tested for preferential introgression of mitonuclear genes and detected evidence for such biased introgression in yellowhammers. Mitonuclear co-introgression can remove post-zygotic incompatibilities between species and may contribute to the continued hybridization between yellowhammers and pine buntings despite their clear morphological and genetic differences. As such, our results highlight the potential ramifications of co-introgression in species evolution.

Introduction

Evolution in eukaryotes is shaped by changes in multiple genomic components that differ in their modes of inheritance: mitochondrial DNA (mtDNA) is usually inherited through the

matrilineal line, autosomes are inherited through both parental lines and sex chromosomes are inherited differentially depending on the sex of both parent and offspring (Avise, 2000). There is often much variation among these genomic components in the degree of genetic differentiation between related populations or species (reviewed in Coyne & Orr, 2004; reviewed in Price, 2008), suggesting that their dynamics differ during the process of speciation of a single species into two or more. This variation can arise through differences in both the rate at which specific DNA sequences evolve and the degree to which different components contribute towards genetic incompatibilities that reduce gene flow between populations. A common pattern observed between speciating taxa is clear differentiation in mtDNA (eg. Hebert et al. 2004; Kerr et al. 2007), moderate differentiation in sex chromosomes (eg. Thornton & Long, 2002; Borge et al. 2005; Lu & Wu, 2005; Harr, 2006; Ruegg et al. 2014; Sackton et al. 2014), and comparatively modest differentiation across autosomes (Harr, 2006; Nadeau et al. 2012; Irwin et al. 2018).

Measures of mtDNA differentiation are often used to identify and classify genetically distinct populations (eg. Hebert et al. 2004; Kerr et al. 2007) and to infer their histories (Moore, 1995; Zink & Barrowclough, 2008). Due to its uniparental inheritance, mtDNA has one quarter the effective population size and coalescence time of autosomal nuclear DNA (Moore, 1995). This characteristic combined with mtDNA's relatively high mutation rate (Lynch et al. 2006) mean that genetic differences arise and fix relatively quickly, creating patterns of clear mtDNA differentiation between recently diverged populations.

Sex chromosomes are another genomic region that often shows higher between-population genetic differentiation compared to autosomes between speciating taxa, in both Z/W (Borge et al. 2005; Ruegg et al. 2014; Sackton et al. 2014) and X/Y systems (Thorton & Long, 2002; Lu & Wu, 2005; Harr, 2006). To explain this "faster Z/X effect," researchers have noted

that, because beneficial recessive mutations on the Z or X chromosome are immediately exposed to selective forces in the heterogametic sex, fixation of these mutations should proceed faster than if the mutations appeared on autosomes (reviewed in Meisel & Connallon, 2013; Irwin, 2018). Also contributing to genetic differentiation on the Z and X chromosomes are the lower effective population sizes of these chromosomes compared to autosomes (Mank et al. 2010; reviewed in Irwin, 2018). A lower effective population size allows for the fixation of a greater number of slightly deleterious mutations due to less effective purifying selection and a larger role of genetic drift. It is likely that both forces—the faster Z/X effect and less effective purifying selection—contribute to the moderate amount of genetic differentiation seen between the sex chromosomes of diverging taxa (Thorton & Long, 2002; Borge et al. 2005; Lu & Wu, 2005; Harr, 2006; Ruegg et al. 2014; Sackton et al. 2014).

Differentiation across autosomes, which tends to be lower than on mtDNA and sex chromosomes, can be highly heterogeneous. In fact, many researchers report "islands of differentiation" on autosomes where peaks of high relative differentiation are found against a background of low relative differentiation (e.g., Harr, 2006; Nadeau et al. 2012; Hejase et al. 2020). Explanations for these "islands" usually invoke reduced gene flow (reviewed in Wu, 2001) and/or repeated bouts of selection (Cruickshank and Hahn, 2014; Irwin et al. 2018). In the former scenario, differentiation peaks are hypothesized to house the loci responsible for reproductive barriers between interacting taxa and, as a result, they are resistant to the gene flow that homogenizes the rest of the nuclear genome. In contrast, explanations invoking repeated selection hypothesize that differentiation islands are areas of the genome that experienced repeated reductions in genetic diversity as a result of selection or selective sweeps in both ancestral and daughter populations.

Despite the general patterns of differentiation discussed above, an increasing number of studies report remarkably low differentiation between populations at what are normally highly divergent genetic components when compared to other genetic regions or observable phenotypes (e.g., Irwin et al. 2009; Yannic et al. 2010; Bryson et al. 2012). In a number of cases, mtDNA shows dramatically low differentiation when compared to differentiation of the nuclear genome, a pattern referred to as "mitonuclear discordance" (reviewed in Toews & Brelsford, 2012). Discordance between marker types may be explained by hybridization and introgression between populations, perhaps due to a selective advantage of the introgressing genetic region. For example, Hulsey et al. (2016) documented low mtDNA differentiation—likely due to introgression—and clear differentiation in nuclear DNA (nucDNA) between two hybridizing cichlid species (Hulsey & García de León, 2013). The researchers further reported high mtDNA differentiation between isolated populations of cichlids at genetic sites associated with thermal tolerance and a significant correlation between mtDNA divergence and water temperature (Hulsey et al. 2016). Altogether, these results suggest that mtDNA introgression produced the discordance seen between marker types and that this outcome was potentially driven by adaptive selection for tolerance of extreme water temperatures.

The hypothesis of adaptive introgression increases in complexity if we consider the potential for coevolution between genomic components. Research investigating coevolution between mitochondrial and nuclear genomes is relatively novel as mtDNA was often treated as a neutral marker in past evolutionary research (Avise, 2000). Nevertheless, recent empirical and theoretical work has provided greater context regarding how mitonuclear coevolution may influence the progression of differentiation and speciation between taxa (Hill, 2019).

Mitonuclear ecology is the study of how forces acting on the mitochondrial and nuclear genomes interact to influence ecological and evolutionary processes (Hill, 2019). Best known for aerobic respiration, the mitochondrion is the site of the electron transport chain (ETC) responsible for oxidative phosphorylation in eukaryotic organisms (reviewed in Ernster & Schatz, 1981). Due to the mitochondrial genome's reduced size of about 37 genes, proper functioning of the ETC as well as transcription, translation and replication of mtDNA is reliant on about 1500 proteins encoded by mitonuclear genes within the nuclear genome (Calvo & Mootha, 2010; Lotz et al. 2014). This interplay between mtDNA and nucDNA implies coevolution between the two genomes such that changes in one places selection on the other for compensatory changes that reduce genetic incompatibility and maintain mitochondrial function (Gershoni et al. 2009; Burton & Barreto, 2012; Hill, 2019). Secondary contact and hybridization between differentiated populations can result in hybrid breakdown due to mismatches between coevolved combinations of mtDNA and mitonuclear genes, contributing to reproductive isolation and eventual speciation of the groups. Yet, introgression of an adaptive mitochondrial haplotype from one population into another could select for similar introgression of compatible alleles at mitonuclear genes (eg. Beck et al. 2015; Morales et al. 2018; Wang et al. 2021). Such co-introgression would act as a homogenizing force and decrease genetic differentiation between populations in both the mitochondrial and nuclear genomes.

The potential for introgression between speciating populations depends on the degree to which they are in geographic contact during their period of differentiation. In many cases, closely related species occur in allopatry, but in others, taxa meet in areas of contact where they may interbreed (reviewed in Coyne & Orr, 2004; reviewed in Price, 2008). Successful hybridization and backcrossing allow for the introduction of genetic variation from one

145 population into the other and for adaptive introgression or co-introgression between taxa at
146 particular genomic regions which can create the discordant differentiation patterns noted in many
147 systems (reviewed in Toews & Brelsford, 2012). To look for evidence of adaptive co-
148 introgression, we must therefore examine systems where two species are or have hybridized
149 previously and where different genomic components show discordant patterns of genetic
150 differentiation.

151 An example of one such system includes the yellowhammer (Passeriformes:
152 Emberizidae: *Emberiza citrinella*) and the pine bunting (*Emberiza leucocephalos*)—an avian
153 species pair thought to have diverged during the Pleistocene glaciations when they were
154 separated on either side of Eurasia by an area of unsuitable habitat (Irwin et al. 2009). These taxa
155 are highly divergent in plumage and moderately divergent in song and ecology (Panov et al.
156 2003; Rubtsov & Tarasov, 2017). Despite their differences, yellowhammers and pine buntings
157 hybridize extensively in a large contact zone in central and western Siberia (Panov et al. 2003;
158 2007; Rubtsov, 2007; Irwin et al. 2009; Rubtsov & Tarasov, 2017). Genomic work has identified
159 mitonuclear discordance between allopatric yellowhammers and pine buntings (Irwin et al. 2009)
160 as they possess almost no mtDNA divergence but show moderate differentiation in nuclear
161 AFLP (Amplified Fragment Length Polymorphism) markers. To explain these results, Irwin et
162 al. (2009) suggested that mtDNA may have introgressed from one species into the other during a
163 previous selective sweep, and this hypothesis was supported by several statistical tests performed
164 on the mtDNA haplotype network. Such mtDNA introgression could select for co-introgression
165 at mitonuclear genes if sizeable genetic differentiation had developed between yellowhammers
166 and pine buntings (Sloan et al. 2017; Hill, 2019; Wang et al. 2021) which is implied by their
167 divergent behaviour, ecology and appearance. Mitonuclear co-introgression and the resulting

lack of mitonuclear incompatibility could facilitate the continued hybridization seen between yellowhammers and pine buntings and prevent the build-up of reproductive isolation and full speciation between these taxa (Hill, 2019).

Here we present the first largescale comparison of DNA sequence variation across the nuclear genomes of allopatric yellowhammers and pine buntings. We address several key questions regarding genetic differentiation in this system. First, does nucDNA differentiation between yellowhammers and pine buntings resemble that of mtDNA (virtually none), that of plumage phenotype (very strong differentiation), or something in between? The earlier AFLP results suggested clear differentiation of nuclear markers between groups (Irwin et al. 2009), but those results were not based on actual DNA sequences. Substantial nuclear differentiation would provide stronger support for the hypothesis that there has been mitochondrial introgression and replacement. Second, what is the structure of differentiation across the nuclear genome? The degree of heterogeneity in differentiation across the genome can be used to test whether adaptive introgression may have occurred in this system, and whether certain regions of the genome (e.g., the sex chromosomes) may be especially important during divergence. Third, is there an over-representation of known mitonuclear genes within putatively introgressing nucDNA regions–a pattern consistent with mitonuclear co-introgression? Evidence of mitonuclear co-introgression and the resulting loss of mitonuclear incompatibility could offer a possible explanation for the extensive hybridization seen between yellowhammers and pine buntings as well as implicate this process as a homogenizing force that counters divergence between these groups.

Materials and Methods

Sampling

We included 109 blood and tissue samples in this study: 53 phenotypic yellowhammers, 42 phenotypic pine buntings, and 14 other members of Emberizidae (one *Emberiza aureola* [yellow-breasted bunting], one *Emberiza calandra* [corn bunting], one *Emberiza cioides* [meadow bunting], one *Emberiza hortulana* [ortolan bunting], four *Emberiza stewarti* [white-capped bunting], and six *Emberiza cirlus* [cirl bunting]) to put variation between yellowhammers and pine buntings into a deeper phylogenetic context (Figure 1A; Table 1; Supplementary Table 1). A total of 91 samples were included in the AFLP analysis of Irwin et al. (2009) while 18 samples were examined for the first time as part of the present research.

When possible, body measurements and photographs were taken of live birds or museum skins. Yellowhammer and pine bunting males were also scored phenotypically and sorted into phenotypic classes based on the protocols presented in Panov et al. (2003) and Rubtsov & Tarasov (2017). Briefly, each male received a score from 0-7 for background plumage colour, the amount of chestnut plumage (vs. yellow or white) at the brow and the amount of chestnut plumage (vs. yellow or white) at the throat. For background colour, birds were assessed on the strength of yellow—ranging from bright yellow to pure white—in head and body plumage that did not show brown or black streaking. Phenotypic scores of 0 are consistent with a phenotypically pure yellowhammer and scores of 7 are consistent with a phenotypically pure pine bunting. Phenotypic classes included: pure citrinella (PC), almost citrinella (SC), citrinella hybrid (CH), yellow hybrid (YH), white hybrid (WH), leucocephalos hybrid (LH), almost leucocephalos (SL) and pure leucocephalos (PL) (Rubtsov & Tarasov, 2017). Unless stated otherwise, any SC and SL individuals that appeared in the allopatric zones were grouped

212 together with PC and PL individuals respectively and treated as phenotypic yellowhammers and
213 phenotypic pine buntings in subsequent analyses (Figure 1B).

214 **DNA extraction and genotyping-by-sequencing**

215 DNA was extracted from samples using a standard phenol-chloroform method. We then
216 divided the DNA samples into four genotyping-by-sequencing (GBS) libraries (Elshire et al.
217 2011). The 109 samples included in this study were sequenced in libraries together with 226
218 yellowhammer, pine bunting and hybrid DNA samples collected near and within the sympatric
219 zone as part of a larger project (Nikelski et al. in prep). The libraries were prepared as per the
220 protocol described by Alcaide et al. (2014) with the modifications specified by Geraldes et al.
221 (2019) except that we maintained a 300-400 bp fragment size during size selection. Paired-end
222 sequencing was completed by Genome Québec using the Illumina HiSeq 4000 system,
223 producing more than 1.2 billion reads, 150 bp in length, across the four GBS libraries.

224 **Genotyping-by-sequencing data filtering**

225 Processing of GBS reads for the samples analyzed in this study was done in conjunction
226 with reads from the samples included in the larger project mentioned above. We processed the
227 reads following Irwin et al. (2016; 2018), as summarized here. Reads were demultiplexed using a
228 custom perl script designed by Baute et al. (2016). Next, reads were trimmed for quality using
229 Trimmomatic version 0.36 (Bolger et al. 2014) with the parameters: TRAILING:3,
230 SLIDINGWINDOW:4:10, MINLEN:30. Trimmed reads were aligned to the zebra finch
231 reference genome (*Taeniopygia guttata* version 3.2.4; Warren et al. 2010) using the program
232 BWA-MEM (Li & Durbin, 2009) and a BAM file of this information was created for each
233 individual using the programs Picard (http://broadinstitute.github.io/picard/) and SAMtools (Li et

al. 2009). Then, BAM files were converted into GVCF files using the HaplotypeCaller command as part of GATK version 3.8 (McKenna et al. 2010). We processed the resulting GVCF files in two ways to create 1) a genome-wide "variant site" VCF file containing information only on variant sites, and 2) a series of chromosome-specific "info site" VCF files containing information on both variant and invariant sites with sufficient coverage.

To create the genome-wide "variant site" VCF file, we used the GenotypeGVCFs command in GATK version 3.8 to identify and isolate single nucleotide polymorphisms (SNPs) among individuals. This command also converted the variant site information into a single VCF file encompassing the entire nuclear genome. Using a combination of VCFtools (Danecek et al. 2011) and GATK, we filtered the VCF file to remove indels and non-biallelic SNPs. We also discarded loci with QD < 2.0, MQ < 40.0, FS > 60.0, SOR > 3.0, or ReadPosRankSum < -8.0. Finally, loci with more than 60% missing genotypes were removed. The average coverage of variable sites in the resulting VCF file was 16.59.

To convert GVCF files into "info site" VCF files, we similarly employed the GenotypeGVCFs command in GATK with the addition of the -allSites and -L flags to retain invariant sites and split the information into chromosome-specific files. The resulting VCF files were filtered using VCFtools and GATK to remove indels, sites with more than two alleles, sites with more than 60% missing genomic data, sites with MQ values lower than 20 and sites with heterozygosities greater than 60% (to avoid potential paralogs). Use of these filters simplified calculations in downstream analyses and ensured that these analyses were restricted to sites with sufficient data.

All following statistical analyses were completed using R version 3.6.2 (R Core Team, 2014).

Variant site analyses

The genome-wide "variant site" VCF file was analyzed using modified versions of the R scripts described in Irwin et al. (2018). A total of 374,780 SNPs were identified among allopatric yellowhammers and pine buntings. For each of these SNPs we calculated sample size, allele frequency, and Weir and Cockerham's F_{ST} (Weir & Cockerham, 1984). Genetic differentiation between yellowhammers and pine buntings was then visualized using a principal components analysis (PCA) generated with the pca command and the svdImpute method to account for any missing genomic data using the pcaMethods package (Stacklies et al. 2007). The PC1 loadings were also graphed as a Manhattan plot using the package qqman (Turner, 2018). Finally, to examine the spread of variant sites across the genome and identify areas of high differentiation, the F_{ST} values of 349,807 SNPs were graphed as a Manhattan plot. The remaining SNPs did not possess known genomic locations and, therefore, could not be included in the plot.

Differentiation across the genome

To thoroughly investigate genomic differentiation between allopatric yellowhammers and pine buntings, we performed further analysis on both variant and invariant loci within "info site" VCF files using R scripts described in Irwin et al. (2018).

We calculated Weir and Cockerham's F_{ST}, between-group nucleotide distance (π_B) and within-group nucleotide diversity (π_W) for nonoverlapping windows of available sequence data across each chromosome. The first window was positioned at the "start" of each chromosome as described in the zebra finch reference genome (Warren et al. 2010). We used a window size of 2000 bp of sequenced data rather than 10,000 bp (as in Irwin et al. 2018), to visualize narrow peaks in relative and absolute differentiation within our dataset.

We developed a new R script to calculate a Tajima's D value (Tajima, 1989) for each of the 2000 bp windows. Values of Tajima's D were used to identify areas of the genome where patterns of variation in yellowhammer and pine bunting populations deviated from models of neutrality. Significantly negative Tajima's D implies that there are more rare alleles in a population than expected under neutrality, likely because of a selective sweep or population expansion following a bottleneck. Significantly positive Tajima's D suggests that there are fewer rare alleles in a population than expected under neutrality, potentially stemming from balancing selection or rapid population contraction.

Phylogenetic comparison with other Emberizidae species

We employed whole-genome averages of π_B between allopatric yellowhammers and allopatric pine buntings as well as among these focal species and six other Emberizidae species (*Emberiza aureola, Emberiza calandra, Emberiza cioides, Emberiza cirlus, Emberiza hortulana and Emberiza stewarti*) to estimate a phylogeny. A list of average π_B values for each species pair was converted into a distance matrix and used to create an unrooted neighbour-joining tree. This tree was constructed using the ape package (Paradis & Schliep, 2019) and the BioNJ algorithm (Gascuel, 1997) with *Emberiza aureola* set as the outgroup (Alström et al. 2008).

Signals of mitonuclear co-introgression

To test for signals of mitonuclear gene introgression between allopatric yellowhammers and pine buntings, we compiled a list of mitonuclear genes and a list of 2000 bp putative introgression windows (hereafter referred to as "introgression windows") and then tested for an association between them. We explain these steps in detail below. If mitonuclear genes were found within introgression windows statistically more often than was expected due to chance, it

would provide support for mitonuclear gene introgression potentially in response to the adaptive mtDNA introgression (Hill, 2019) hypothesized to have occurred in this system (Irwin et al. 2009).

To start, we created a list of mitonuclear genes to analyze for signals of introgression. We chose mitonuclear genes that were protein-coding and whose protein products interacted directly with mtDNA or an immediate product of the mitochondrial genome (i.e. protein or RNA). For these nuclear-encoded genes, any change in mtDNA including those caused by introgression would likely cause selection for co-introgression of compatible alleles (Gershoni et al. 2009; Burton & Barreto, 2012; Hill, 2019). Mitonuclear genes that met these criteria included those that encode protein subunits of ATP synthase or the first, third and fourth complex of the ETC, assembly and ancillary proteins involved in the formation of the ETC, or proteins that are part of the transcription, translation or DNA replication machinery within the mitochondria. This list of genes was created using information from Figure 2.3 and Table 2.1 in Hill (2019). After removing any genes that were not annotated in the zebra finch reference genome or that lacked a specific location on the reference genome, a total of 134 mitonuclear genes remained for analysis (Supplementary Table 2).

Next, we identified introgression windows across the genome as those possessing both a low Tajima's D value and a low π_B value. Low π_B indicates high similarity between the nucleotide sequences of two groups as would be expected if mitonuclear gene alleles had introgressed from one taxon into the other. Low Tajima's D suggests a past selective sweep within a population which would also be expected if an adaptive mitonuclear allele had introgressed from a separate taxon and swept throughout the receiving population. For this analysis, our quantitative criteria for an introgression window were a Tajima's D value within

the lowest 5% of the available windowed values and a π_B value within the lowest 30% of the available windowed values. Out of the 7187 windows described across the genome, 244 introgression windows were identified for yellowhammers and 222 introgression windows were identified for pine buntings. As well, of the introgression windows identified in yellowhammer and pine bunting populations, 71 were shared between the taxa. It should be noted that sharing of some introgression windows is expected given that the contribution of π_B to window selection was identical for both taxa (in contrast, Tajima's D was calculated separately for yellowhammers and pine buntings).

Following window classification, we employed a custom R script to determine how many mitonuclear genes occurred within introgression windows. To do this, we identified the genomic centre position of each mitonuclear gene as well as the average genomic position of each of the genomic windows. We then calculated the absolute difference between mitonuclear gene centres and average window positions. Mitonuclear genes were assumed to occur within whatever window minimized this difference. With this information, we were able to determine the number of mitonuclear genes that occurred within the introgression windows of each taxon.

The number of mitonuclear genes within introgression windows were compared to what would be expected if these genes were distributed randomly across the genome using separate two-tailed binomial tests for yellowhammers and pine buntings. Because genes are often not distributed randomly and may appear more densely packed in certain genomic regions (International Chicken Genome Sequencing Consortium, 2004), we also conducted a Fisher's Exact test for both yellowhammers and pine buntings to determine whether the proportion of mitonuclear genes within introgression windows was significantly different from what would be expected based on the total proportion of protein coding genes appearing within these windows.

Results

When comparing allopatric yellowhammers and pine buntings, following filtering we identified 374,780 variable SNPs within our "variant site" VCF file and 13,703,455 invariant and 699,122 variant sites across thirty autosomes and the Z chromosome within our "info site" VCF files. In the latter "info site" files, we designated a total of 7187 genomic windows (of 2000 sequenced bp each) across the genome, with each window covering an average distance of about 139 kilobases.

Phylogenetic comparison with other Emberizidae species

An unrooted neighbour-joining tree of average π_B values between yellowhammers, pine buntings and six other Emberizidae species (Figure 2) depicted similar species relationships as were identified previously using mitochondrial markers (Alström et al. 2008; Irwin et al. 2009). As well, similar relative branch lengths between taxa were recovered with the exception of that between yellowhammers and pine buntings. In terms of the relative genetic distance (π_B) between yellowhammers and pine buntings compared to the distance between each of those and *E. stewarti*, nuclear genetic distance was 11.4 times greater than mitochondrial genetic distance. This corroborates the presence of mitonuclear discordance between the taxa where nucDNA is much more deeply diverged than mtDNA, supporting the hypothesis of an extended period of divergence between yellowhammers and pine buntings followed by mtDNA introgression.

Overall genetic differentiation

Based on 374,780 SNPs considered all together, our genome-wide F_{ST} estimate was 0.0232 between allopatric yellowhammers and pine buntings. Despite this low average, a PCA based on the same SNP genotypes separated yellowhammers and pine buntings into tight genetic

clusters (Figure 3). PC1 explained 3.6% of the variation among individuals while PC2 explained 2.9% of the variation. Two pine buntings were outliers along PC1, while the remaining yellowhammers and pine buntings separated into distinct clusters mainly along PC2. Further investigation into these outliers revealed that they were males from the same location. A kinship analysis completed as part of a separate study did not find close kinship between the two pine buntings that could explain their position as outliers (Nikelski et al. in prep). An examination of the PC1 loadings for each of the SNPs revealed that the signal for the PC1 positioning was broadly distributed across the genome, rather than being concentrated in a few specific regions (Supplementary Figure 1). To explore the causes of these outliers, we temporarily removed one of them and re-ran the PCA. This caused the other outlier to fall into the pine bunting cluster, but did reveal a further yellowhammer outlier (Supplementary Figure 2). Removal of this yellowhammer outlier in addition to one member of the pine bunting outlier pair in turn revealed another yellowhammer outlier (Supplementary Figure 3). It is unclear what is responsible for these outliers, but the distinct yellowhammer and pine bunting genetic clusters remained intact in all the PCAs considered.

Differentiation across the genome

Relative differentiation between allopatric yellowhammers and pine buntings was highly heterogeneous across the nuclear genome with peaks in F_{ST} seen on most of the larger chromosomes (Figures 4, 5; Supplementary Figure 4). Chromosome Z in particular showed a large peak in F_{ST} with several SNPs possessing values close to one. In fact, F_{ST} for the Z chromosome was 0.1246—more than five times larger than the genome-wide F_{ST}.

Patterns of between-group nucleotide diversity (π_B) and within-group nucleotide diversity (π_W) were also heterogenous across the genome and comparable to each other in

magnitude: genome-wide π_B = 0.0041; genome-wide π_W for both taxa= 0.0040 (Figure 5; Supplementary Figure 4). Because between-group and within-group nucleotide diversity are so intimately related in their evolution and calculation, it is expected that windowed averages of these two statistics will show a highly positive relationship. In fact, most windowed π_B and π_W averages fell near a 1:1 association line (Figure 6) which is equivalent to no or little differentiation. However, some genomic windows showed much reduced π_W compared to π_B; these were the windows with high F_{ST}. Additionally, we detected a weak negative correlation between the windowed averages of F_{ST} and π_B (Spearman's Rank Correlation: -0.1196, $p < 2.2 \times 10^{-16}$; Figure 7) as is hypothesized if peaks in relative differentiation are products of repeated selective events (Cruickshank & Hahn, 2014; Irwin et al. 2018).

Finally, we found that Tajima's D varied across the genome but was mostly negative (Figure 5; Supplementary Figure 4), consistent with a history of population growth and/or selective sweeps. The average genome-wide Tajima's D was similar between populations: -1.377 for yellowhammers and -1.335 for pine buntings.

Signals of mitonuclear co-introgression

Of the 7187 genomic windows identified across the nuclear genome, we classified 244 as introgression windows within yellowhammers and 222 as introgression windows within pine buntings (Table 2). Average values of π_B and Tajima's D in yellowhammer introgression windows were 0.0016 and -2.3751 respectively, and 0.0019 and -2.3369 in pine buntings respectively.

Nine mitonuclear genes—6.7% of the 134 mitonuclear genes considered—appeared within yellowhammer introgression windows (Table 2). This finding was significant in a two-

414 tailed binomial test (p = 0.04952) indicating that mitonuclear genes appeared in yellowhammer
415 introgression windows more often than would be expected if they were assigned to windows
416 randomly. However, this finding was not significant in a Fisher's Exact test (p = 0.1311) which
417 takes into account the differing densities of genes across the nuclear genome. Four mitonuclear
418 genes appeared within pine bunting introgression windows—3.0% of the genes considered. This
419 result was statistically insignificant in both a two-tailed binomial test (p = 1) and a Fisher's Exact
420 test (p = 1) indicating that mitonuclear genes did not appear in pine bunting introgression
421 windows more often than would be expected due to chance. Overall, the significant signal of
422 introgression in yellowhammers and insignificant signal of introgression in pine buntings could
423 indicate that mitonuclear gene introgression—if it occurred—was biased in the direction of pine
424 buntings into yellowhammers.

425 The nine mitonuclear genes that appeared within yellowhammer introgression windows
426 are: APOPT1, COX5A, COX17, MRPL1, MRPL27, MRPL32, NDUFC1, mtSSB, UQCR11
427 (Table 3). Three of these genes encode protein subunits of the mitochondrial ribosome, three
428 encode structural subunits of the ETC, two encode assembly factors of the ETC and one encodes
429 a single-stranded DNA-binding protein involved in mtDNA replication. All putatively
430 introgressed genes appear on separate autosomes except for two genes that appear on
431 chromosome 4. Interestingly, three of the five putatively introgressed genes associated with the
432 ETC are specifically associated with complex IV.

433 The four mitonuclear genes that appeared within pine bunting introgression windows are:
434 ATP5H5I, COX5A, MRPL2 and NDUFB4 (Table 4). All four genes appeared on separate
435 autosomes with three of these genes encoding structural subunits of the ETC and one encoding a
436 protein subunit of the mitochondrial ribosome. The COX5A gene, which encodes a structural

437 subunit of ETC complex IV, was found in both yellowhammer and pine bunting introgression
438 windows.

439

440 ***Discussion***

441 Yellowhammers and pine buntings show negligible mtDNA differentiation (Irwin et al.
442 2009) but are well differentiated phenotypically (Panov et al. 2003, Rubtsov & Tarasov, 2017).
443 Prior to this study, a possible explanation for this pattern was simply rapid phenotypic evolution
444 between two genetically similar sister taxa. Our analysis of nucDNA variation has shown clear
445 separation of allopatric yellowhammers and pine buntings, with strong differentiation peaks in
446 specific parts of the nuclear genome. This result points to these taxa experiencing a long period
447 of separate evolution followed by the hybridization now observed within a large contact zone in
448 western and central Siberia. These results combined with our phylogenetic analysis showing a
449 longer branch length between yellowhammers and pine buntings based on nuclear markers—
450 when compared to a phylogeny based on mtDNA (Irwin et al. 2009)—support recent mtDNA
451 introgression and mitochondrial haplotype replacement in this system likely driven by selection.
452 Our analyses also provided some evidence for the disproportionate introgression of mitonuclear
453 genes between taxa which is consistent with co-introgression discussed in current mitonuclear
454 theory (Hill, 2019).

455 Though genetically distinct, the genome-wide F_{ST} between allopatric yellowhammers and
456 pine buntings (0.0232) was comparable to or sometimes lower than the averages seen between
457 avian subspecies (e.g., subspecies of barn swallow: 0.017-0.026 [Scordato et al. 2017]; myrtle
458 warbler and Audubon's warbler: 0.077-0.106 [Irwin et al. 2018]; yellow- and red-shafted

northern flickers: 0.098 [Manthey et al. 2016]). This low genome-wide F_{ST} contrasts with the moderate F_{ST} averages reported from an analysis of 63 AFLP markers performed on the same populations: 0.078 based on allele frequencies and 0.140 based on band frequencies (Irwin et al. 2009). The present study reveals that relative differentiation was highly heterogeneous across the nuclear genome with F_{ST} peaks on various chromosomes. It is possible that the previous AFLP analysis captured a disproportionate number of loci within these differentiation peaks, thereby inflating F_{ST} estimates. This comparison highlights the caution that should be taken when interpreting genome-wide averages as highly variable genetic differentiation landscapes can cause large variability in F_{ST} estimates when they are based on a limited number of loci.

The F_{ST} peaks seen between yellowhammers and pine buntings on larger autosomes and most significantly on the Z chromosome are consistent with the "islands of differentiation" often noted in comparisons of other closely related taxa (Harr, 2006; Nadeau et al. 2012; Irwin et al. 2018). In contrast to these islands, the large regions of close similarity in π_B and π_W suggests high gene flow between taxa at those regions. This scenario is consistent with the observed extensive hybridization between these taxa (Panov et al. 2003; 2007; Rubtsov, 2007; Rubtsov & Tarasov, 2017). Nevertheless, the high F_{ST} regions, those with much reduced π_W compared to π_B, indicate that they have had low gene flow presumably as a result of divergent selection. It is unlikely that this pattern can be explained by genetic drift over an extended period of geographic separation, as this would result in most genomic regions deviating slightly from $\pi_B = \pi_W$ congruence rather than the observed pattern of extreme heterogeneity. Instead, the pattern suggests that selection acted in a way that lowered π_W relative to π_B within "islands of differentiation". Considering that high F_{ST} regions were associated with relatively low values of π_B, we propose that differentiation islands in this system are most consistent with a model

482 invoking repeated bouts of selection that lower nucleotide diversity (Cruickshank & Hahn, 2014;
483 Irwin et al. 2018). A sweep-before-differentiation model (Irwin et al. 2018) where F_{ST} peaks are
484 produced by adaptive selective sweeps between populations followed by adaptive selection at the
485 same regions in local populations is particularly in line with the extensive hybridization presently
486 observed between yellowhammers and pine buntings.

487 Of the "islands of differentiation" identified between taxa, the tallest and widest was
488 found on the Z chromosome. Greater differentiation on the Z chromosome compared to
489 autosomes is a common observation when comparing closely related species (Borge et al. 2005;
490 Ruegg et al. 2014; Sackton et al. 2014) and is consistent with the "faster Z/X effect" that has
491 been explained by less efficient purifying selection and/or more positive selection on this
492 chromosome (Mank et al. 2010; reviewed in Meisel & Connallon, 2013; reviewed in Irwin,
493 2018). However, the large regions of the Z chromosome that have F_{ST} values near zero suggests
494 that additional factors are involved in producing the large and wide island of differentiation on
495 the Z.

496 One possible explanation for a large differentiation island could be that it corresponds
497 with an area of low recombination—a region of connected loci that tend to be inherited together,
498 leading to linked selection of nearby loci. Strong divergent selection acting on one SNP would
499 act similarly on all the loci that are linked to it such that a wide, highly divergent genomic block
500 would become fixed and appear as an "island" between taxa (reviewed in Cutter & Payseur,
501 2013). Areas of low recombination and linkage are often associated with inversion
502 polymorphisms (reviewed in Smukowski & Noor, 2011) as different orientations of an inversion
503 experience little successful recombination (reviewed in Kirkpatrick, 2010). An exploration of a
504 potential chromosomal inversion within the yellowhammer and pine bunting system is being

505 investigated as part of a separate study and is supported by preliminary evidence (Nikelski et al.
506 in prep).

507 While numerous "islands of differentiation" were observed between yellowhammers and
508 pine buntings implying moderate genetic divergence between them, mtDNA introgression has
509 the potential to homogenize their nuclear genomes at mitonuclear genes by selecting for co-
510 introgression of compatible alleles (Beck et al. 2015; Sloan et al. 2017; Morales et al. 2018).
511 Consistent with this idea, a two-tailed binomial test supported preferential introgression of
512 mitonuclear genes in allopatric yellowhammers. Because a comparable signal of introgression
513 was not found in allopatric pine buntings, we suggest that mitonuclear co-introgression could
514 have occurred in the direction of pine buntings into yellowhammers. Yet, these results must be
515 interpreted with caution due to limitations in introgression window identification. Because we
516 employed reduced-representation sequencing that only captures a small portion of the nuclear
517 genome, we have limited resolution in detecting signals of introgression over narrow genomic
518 regions. This may have contributed to the variation we saw in the statistical significance of
519 mitonuclear gene introgression depending on whether gene densities were considered.
520 Nevertheless, the fact that a significant signal of introgression was detected despite limitations is
521 intriguing especially when considered in conjunction with the identities of the mitonuclear genes
522 found in introgression windows.

523 Three of the mitonuclear genes within yellowhammer introgression windows and three
524 within pine bunting introgression windows encoded structural subunits of the ETC. The ETC is
525 broken into five protein complexes which, through a series of enzymatic reactions, perform
526 oxidative phosphorylation to produce ATP necessary for organism survival (reviewed in Ernster
527 & Schatz, 1981). Four of the five ETC complexes are made up of subunits encoded by both the

nuclear and mitochondrial genome (Hill, 2019) and correct fit between differentially encoded subunits is essential for the flow of electrons and protons across the ETC. To put this in perspective, changing even a single amino acid in one subunit can significantly disrupt its ability to interact with other subunits within a ETC complex (eg. Gershoni et al. 2014). Because of the tight interactions within complexes and the consequences of subunit incompatibility, introgression of mtDNA is expected to select for co-introgression of mitonuclear genes encoding ETC structural subunits. Such co-introgression has been detected between differentially adapted populations of eastern yellow robin where mtDNA introgression between populations was followed by similar introgression of mitonuclear genes encoding subunits of complex I (Morales et al. 2018) and between different species of *Drosophila* where introgression and replacement of the mtDNA of one species during hybridization selected for co-introgression of genes that encode subunits of complex IV (Beck et al. 2015).

Of the ETC complexes, complex IV showed the strongest signal of co-introgression in the yellowhammer and pine bunting system. Three of the genes within yellowhammer introgression windows and one gene within pine bunting introgression windows were associated with this complex. Interestingly, gene COX5A—a structural subunit of complex IV—appeared in both sets of introgression windows. It is unlikely that this gene introgressed in both directions, but it is possible that COX5A adaptively swept in both populations. In this situation, a particularly adaptive allele may have appeared in one species and swept to high frequency before co-introgressing into the other species following mtDNA introgression. The COX5A gene was also one of the subunits that co-introgressed in the *Drosophila* example discussed above (Beck et al. 2015) lending some support to its particular importance to mitonuclear compatibility. More generally, complex IV is often used as a model for studying mitonuclear interactions due to its

551 distinctive structure of a core of mtDNA-encoded subunits surrounded by nucDNA-encoded
552 subunits (Saraste, 1999). With such an excess of mitonuclear interactions, incompatibility
553 involving complex IV has been investigated and detected in several systems including within
554 primate xenomitochondrial cybrids (Barrientos et al. 2000) and between different species of
555 *Drosophila* (Sackton et al. 2003). Furthermore, work by Osada & Akashi (2012) has provided
556 strong evidence for compensatory co-evolution between mitonuclear genes related to complex
557 IV and mtDNA among primates particularly at interacting amino acids of differentially encoded
558 subunits. Altogether, these results suggest a crucial role for complex IV in mitonuclear co-
559 evolution as it may relate to divergence and speciation between taxa.

560 Another group of mitonuclear genes that appeared to preferentially introgress within the
561 yellowhammer and pine bunting system were those encoding subunits of the mitoribosome**.**
562 Unlike the protein-protein interactions occurring within ETC complexes, mitonuclear
563 interactions in the mitoribosome are between nuclear-encoded proteins and mitochondrial-
564 encoded RNA (Hill,. 2019). Protein subunits associate closely with rRNA during the formation
565 of a mitoribosome, but also interact with mRNA and tRNA during the synthesis of mitochondrial
566 proteins (Greber & Ban, 2016). Currently, research is limited on the extent and importance of
567 interactions between mitoribosomal subunits and mitochondrial RNA. However, the fact that
568 interactions between components are extensive and necessary for the synthesis of the
569 mitochondrial proteins suggests close co-evolution between mtDNA and genes encoding
570 mitoribosomal subunits that could strongly select for mitonuclear co-introgression following
571 mtDNA introgression.

572 In summary, yellowhammers and pine buntings are sister taxa that are divergent in
573 appearance, song, and ecology (Panov et al. 2003; Rubtsov & Tarasov, 2017) yet vary in their

574 genomic differentiation from virtually none (at the mitochondrial genome) to nearly fixed (the
575 differentiation peak on the Z chromosome). These patterns are best explained by a period of
576 differentiation while geographically separated, followed by hybridization and introgression. We
577 found some evidence of mitonuclear gene introgression in the direction of pine buntings into
578 yellowhammers that is consistent with mitonuclear co-introgression. This occurred preferentially
579 in mitonuclear genes encoding structural components of both the ETC and the mitoribosome,
580 potentially due to mitonuclear incompatability. Mitonuclear incompatibilities are thought to
581 represent an important post-zygotic reproductive barrier between taxa (Gershoni et al. 2009;
582 Burton & Barreto, 2012; Hill, 2019), meaning mitonuclear co-introgression has the potential to
583 weaken species boundaries. Support for such breakdown may be seen in the extensive and
584 dynamic hybrid zone between yellowhammers and pine buntings (Panov et al. 2003; 2007;
585 Rubtsov, 2007; Rubtsov & Tarasov, 2017). Further, careful examination of genetic
586 differentiation and reproductive barriers within the yellowhammer and pine bunting hybrid zone
587 would shed light on the possibility of their merging in the future. As well, the inclusion of
588 analyses that compare mtDNA and mitonuclear gene differentiation in a wider range of systems
589 would help to clarify the potentially important role that mitonuclear interactions play in the
590 merging or diverging of species.

591

592 ***Author contributions:***

593 E. N., D.I., and A.S.R. conceived of this study. A.S.R. collected samples. E. N. and A.S.R.
594 completed molecular techniques. E.G.M.N. conducted data analysis and wrote this manuscript
595 with input from D.I. and A.S.R.

Acknowledgements:

For providing valuable feedback, we thank Dolph Schluter, Eric Taylor, Judith Mank, Elizabeth Natola, Rashika Ranasinghe, Kenneth Askelson, Finola Fogarty, Quinn McCallum, Ana Barreira, Jamie Clarke, Armando Geraldes and Jessica Irwin. For their kindness and support during field work, we thank the Tazeev family and Madelyn Ore. For providing additional samples, we thank The Bell Museum, The Burke Museum of Natural History and Culture, The Field Museum, The State Darwin Museum, The Swedish Museum of Natural History, The Zoological Museum of the Zoological Institute of the Russian Academy of Sciences, the Zoological Museum of the University of Copenhagen and their accompanying personnel. Major research funding was provided by the Natural Sciences and Engineering Research Council of Canada (NSERC CGSM award to E.N, Discovery Grants RGPIN-2017-03919 and RGPAS-2017-507830 awarded to D.I.) and by the Werner and Hildegard Hesse research awards (Research award in Ornithology and Fellowship in Ornithology awarded to E.G.M.N. by the University of British Columbia).

Data Accessibility Statement:

Raw DNA sequencing reads will be made available on the NBCI Sequence Read Archive upon publication acceptance. Read processing codes, barcodes, genotype data and R codes associated with statistical analyses will be made available on Dryad upon publication acceptance.

Conflict of Interest Statement:

None declared

Bibliography

Alcaide, M., Scordato, E. S. C., Price, T. D., & Irwin, D. E. (2014). Genomic divergence in a ring species complex. *Nature, 511*(7507), 83-85. doi:10.1038/nature13285

Alström, P., Olsson, U., Lei, F., Wang, H., Gao, W., & Sundberg, P. (2008). Phylogeny and classification of the old world *Emberizini* (*Aves, Passeriformes*). *Molecular Phylogenetics and Evolution, 47*(3), 960-973. doi:10.1016/j.ympev.2007.12.007

Avise, J. C. (2000). Phylogeography: The history and formation of species. Harvard University Press.

Barrientos, A., Müller, S., Dey, R., Wienberg, J., & Moraes, C. T. (2000). Cytochrome c oxidase assembly in primates is sensitive to small evolutionary variations in amino acid sequence. *Molecular Biology and Evolution, 17*(10), 1508-1519. https://doi.org/10.1093/oxfordjournals.molbev.a026250

Baute, G. J., Owens, G. L., Bock, D. G., & Rieseberg, L. H. (2016). Genome-wide genotyping-by-sequencing data provide a high-resolution view of wild *Helianthus* diversity, genetic structure, and interspecies gene flow. *American Journal of Botany, 103*(12), 2170-2177. doi:10.3732/ajb.1600295

Beck, E. A., Thompson, A. C., Sharbrough, J., Brud, E., & Llopart, A. (2015). Gene flow between *Drosophila yakuba* and *Drosophila santomea* in subunit V of cytochrome c oxidase: A potential case of cytonuclear cointrogression. *Evolution, 69*(8), 1973-1986. doi:10.1111/evo.12718

Bolger, A. M., Lohse, M., & Usadel, B. (2014). Trimmomatic: A flexible trimmer for Illumina sequence data. *Bioinformatics, 30*(15), 2114-2120. doi:10.1093/bioinformatics/btu170

Borge, T., Webster, M. T., Andersson, G., & Saetre, G. (2005). Contrasting patterns of polymorphism and divergence on the Z chromosome and autosomes in two *Ficedula* flycatcher species. *Genetics, 171*(4), 1861-1873. doi:10.1534/genetics.105.045120

Burton, R. S., & Barreto, F. S. (2012). A disproportionate role for mtDNA in Dobzhansky–Muller incompatibilities? *Molecular Ecology, 21*(20), 4942-4957. doi:10.1111/mec.12006

Bryson, J., Robert W, De Oca, A. N., Jaeger, J. R., & Riddle, B. R. (2010). Elucidation of cryptic diversity in a widespread Nearctic treefrog reveals episodes of mitochondrial gene capture as frogs diversified across a dynamic landscape. *Evolution, 64*(8), 2315-2330. https://doi.org/10.1111/j.1558-5646.2010.01014.x

Calvo, S. E., & Mootha, V. K. (2010). The mitochondrial proteome and human disease. *Annual Review of Genomics and Human Genetics, 11*(1), 25-44. doi:10.1146/annurev-genom-082509-141720

Coyne, J. A., & Orr, H. A. (2004). *Speciation*. Sinauer Associates.

Cruickshank, T. E., & Hahn, M. W. (2014). Reanalysis suggests that genomic islands of speciation are due to reduced diversity, not reduced gene flow. *Molecular Ecology, 23*(13), 3133-3157. doi:10.1111/mec.12796

Cutter, A. D., & Payseur, B. A. (2013). Genomic signatures of selection at linked sites: Unifying the disparity among species. *Nature Reviews. Genetics, 14*(4), 262-274. doi:10.1038/nrg3425

Danecek, P., Auton, A., Abecasis, G., Albers, C. A., Banks, E., DePristo, M. A., Handsaker, R. E., Lunter, G., Marth, G. T., Sherry, S. T., McVean, G., Durbin, R. & 1000 Genomes Project Analysis Group. (2011). The variant call format and VCFtools. *Bioinformatics, 27*(15), 2156-2158. doi:10.1093/bioinformatics/btr330

Elshire, R. J., Glaubitz, J. C., Sun, Q., Poland, J. A., Kawamoto, K., Buckler, E. S., & Mitchell, S. E. (2011). A robust, simple genotyping-by-sequencing (GBS) approach for high diversity species. *PloS One, 6*(5), e19379. doi:10.1371/journal.pone.0019379

Ernster, L., & Schatz, G. (1981). Mitochondria: A historical review. *The Journal of Cell Biology, 91*(3), 227s-255s. doi:10.1083/jcb.91.3.227s

687 Gascuel, O. (1997). BIONJ: An improved version of the NJ algorithm based on a simple model
688 of sequence data. *Molecular Biology and Evolution, 14*(7), 685-695.
689 doi:10.1093/oxfordjournals.molbev.a025808

690

691 Geraldes, A., Askelson, K. K., Nikelski, E., Doyle, F. I., Harrower, W. L., Winker, K., & Irwin,
692 D. E. (2019). Population genomic analyses reveal a highly differentiated and endangered
693 genetic cluster of northern goshawks (*Accipiter gentilis laingi*) in Haida Gwaii.
694 *Evolutionary Applications, 12*(4), 757-772. doi:10.1111/eva.12754

695

696 Gershoni, M., Levin, L., Ovadia, O., Toiw, Y., Shani, N., Dadon, S., Barzilai, N., Bergman, A.,
697 Atzmon, G., Wainstein, J., Tsur, A., Nijtmans, L. G. J., Glaser, B., & Mishmar, D.
698 (2014). Disrupting mitochondrial-nuclear coevolution affects OXPHOS complex I
699 integrity and impacts human health. *Genome Biology and Evolution, 6*(10), 2665-2680.
700 https://doi.org/10.1093/gbe/evu208

701

702 Gershoni, M., Templeton, A. R., & Mishmar, D. (2009). Mitochondrial bioenergetics as a major
703 motive force of speciation. *Bioessays, 31*(6), 642-650. doi:10.1002/bies.200800139

704

705 Greber, B. J., & Ban, N. (2016). Structure and function of the mitochondrial ribosome. *Annual*
706 *Review of Biochemistry, 85*(1), 103-132. doi:10.1146/annurev-biochem-060815-014343

707

708 Harr, B. (2006). Genomic islands of differentiation between house mouse subspecies. *Genome*
709 *Research, 16*(6), 730-737. doi:10.1101/gr.5045006

710

711 Hebert, P. D., Penton, E. H., Burns, J. M., Janzen, D. H., & Hallwachs, W. (2004). Ten species
712 in one: DNA barcoding reveals cryptic species in the neotropical skipper butterfly
713 *Astraptes fulgerator*. *Proceedings of the National Academy of Sciences*, *101*(41), 14812-
714 14817. doi:10.1073/pnas.0406166101

715

716 Hejase, H. A., Salman-Minkov, A., Campagna, L., Hubisz, M. J., Lovette, I. J., Gronau, I., &
717 Siepel, A. (2020). Genomic islands of differentiation in a rapid avian radiation have been
718 driven by recent selective sweeps. *Proceedings of the National Academy of*
719 *Sciences*, *117*(48), 30554–30565. doi:10.1073/pnas.2015987117
720

721 Hill, G. E. (2019). *Mitonuclear Ecology* (First ed.). Oxford University Press.

722

723 Hulsey, C. D., Bell, K. L., García-de-León, F. J., Nice, C. C., & Meyer, A. (2016). Do relaxed
724 selection and habitat temperature facilitate biased mitogenomic introgression in a
725 narrowly endemic fish? *Ecology and Evolution, 6*(11), 3684- 3698.
726 https://doi.org/10.1002/ece3.2121

727

728 Hulsey, C. D., & García-de-León, F. J. (2013). Introgressive hybridization in a trophically
729 polymorphic cichlid. *Ecology and Evolution, 3*(13), 4536-4547.
730 https://doi.org/10.1002/ece3.841

731

732 International Chicken Genome Sequencing Consortium. (2004). Sequence and comparative
733 analysis of the chicken genome provide unique perspectives on vertebrate evolution.
734 *Nature, 432*(7018), 695-716. doi:10.1038/nature03154

735

736 Irwin, D. E. (2018). Sex chromosomes and speciation in birds and other ZW systems. *Molecular*
737 *Ecology, 27*(19), 3831-3851. doi:10.1111/mec.14537

738

739 Irwin, D. E., Alcaide, M., Delmore, K. E., Irwin, J. H., & Owens, G. L. (2016). Recurrent
740 selection explains parallel evolution of genomic regions of high relative but low absolute
741 differentiation in a ring species. *Molecular Ecology, 25*(18), 4488-4507.
742 doi:10.1111/mec.13792

743

744 Irwin, D. E., Milá, B., Toews, D. P. L., Brelsford, A., Kenyon, H. L., Porter, A. N., Grossen, C.,
745 Delmore, K. E., Alcaide, M., & Irwin, J. H. (2018). A comparison of genomic islands of
746 differentiation across three young avian species pairs. *Molecular Ecology, 27*(23), 4839-
747 4855. doi:10.1111/mec.14858

748

749 Irwin, D. E., Rubtsov, A. S., & Panov, E. N. (2009). Mitochondrial introgression and
750 replacement between yellowhammers (*Emberiza citrinella*) and pine buntings (*Emberiza*
751 *leucocephalos*) (Aves: Passeriformes). *Biological Journal of the Linnean Society, 98*(2),
752 422-438. doi:10.1111/j.1095-8312.2009.01282.x

753

754 Kerr, K. C. R., Stoeckle, M. Y., Dove, C. J., Weigt, L. A., Francis, C. M., & Hebert, P. D. N.
755 (2007). Comprehensive DNA barcode coverage of North American birds. *Molecular*
756 *Ecology Notes, 7(*4), 535-543. doi:10.1111/j.1471-8286.2007.01670.x

757

758 Kirkpatrick, M. (2010). How and why chromosome inversions evolve. *PLoS Biology, 8*(9),
759 e1000501. doi:10.1371/journal.pbio.1000501

Li, H., & Durbin, R. (2009). Fast and accurate short read alignment with Burrows-Wheeler transform. *Bioinformatics, 25*(14), 1754-1760. doi:10.1093/bioinformatics/btp324

Li, H., Handsaker, B., Wysoker, A., Fennell, T., Ruan, J., Homer, N., Marth, G., Abecasis, G., & Durbin, R. (2009). The sequence alignment map format and SAMtools. *Bioinformatics, 25*(16), 2078-2079. doi:10.1093/bioinformatics/btp352

Lotz, C., Lin, A. J., Black, C. M., Zhang, J., Lau, E., Deng, N., Wang, Y., Zong, N. C., Choi, J. H., Xu, T., Liem, D. A., Korge, P., Weiss, J. N., Hermjakob, H., Yates, J. R., III., Apweiler, R., & Ping, P. (2014). Characterization, design, and function of the mitochondrial proteome: From organs to organisms. *Journal of Proteome Research, 13*(2), 433-446. doi:10.1021/pr400539j

Lu, J., & Wu, C. (2005). Weak selection revealed by the whole-genome comparison of the X chromosome and autosomes of human and chimpanzee. *Proceedings of the National Academy of Sciences, 102*(11), 4063-4067. doi:10.1073/pnas.0500436102

Lynch, M., Koskella, B., & Schaack, S. (2006). Mutation pressure and the evolution of organelle genomic architecture. *Science, 311*(5768), 1727-1730. doi:10.1126/science.1118884

Mank, J. E., Nam, K., & Ellegren, H. (2010). Faster-Z evolution is predominantly due to genetic drift. *Molecular Biology and Evolution, 27*(3), 661-670. doi:10.1093/molbev/msp282

Manthey, J. D., Geiger, M., & Moyle, R. G. (2017). Relationships of morphological groups in the northern flicker superspecies complex (*Colaptes auratus* & *C. chrysoides*). *Systematics and Biodiversity, 15*(3), 183-191. https://doi.org/10.1080/14772000.2016.1238020

McKenna, A., Hanna, M., Banks, E., Sivachenko, A., Cibulskis, K., Kernytsky, A., Garimella, K., Altshuler, D., Gabriel, S., Daley, M., & DePristo, M. A. (2010). The genome analysis toolkit: A MapReduce framework for analyzing next-generation DNA sequencing data. *Genome Research, 20*(9), 1297-1303. doi:10.1101/gr.107524.110

Meisel, R. P., & Connallon, T. (2013). The faster-X effect: Integrating theory and data. *Trends in Genetics, 29*(9), 537-544. doi:10.1016/j.tig.2013.05.009

Moore, W. S. (1995). Inferring phylogenies from mtDNA variation: Mitochondrial-gene trees versus nuclear-gene trees. *Evolution, 49*(4), 718-726. doi:10.2307/2410325

Morales, H. E., Pavlova, A., Amos, N., Major, R., Kilian, A., Greening, C., & Sunnucks, P. (2018). Concordant divergence of mitogenomes and a mitonuclear gene cluster in bird lineages inhabiting different climates. *Nature Ecology & Evolution, 2*(8), 1258-1267. doi:10.1038/s41559-018-0606-3

Nadeau, N. J., Whibley, A., Jones, R. T., Davey, J. W., Dasmahapatra, K. K., Baxter, S. W., Quail, M. A., Joron, M., Ffrench-Constant, R. H., Blaxter, M. L., Mallet, J., & Jiggins, C. D. (2012). Genomic islands of divergence in hybridizing *Heliconius* butterflies identified by large-scale targeted sequencing. *Philosophical Transactions of the Royal Society B: Biological Sciences, 367*(1587), 343-353. doi:10.1098/rstb.2011.0198

Osada, N., & Akashi, H. (2012). Mitochondrial-nuclear interactions and accelerated compensatory evolution: Evidence from the primate cytochrome c oxidase complex. *Molecular Biology and Evolution, 29*(1), 337-346. https://doi.org/10.1093/molbev/msr211

Panov, E. N., Rubtsov, A. A., & Monzikov, D. G. (2003). Hybridization between yellowhammer and pine bunting in Russia. *Dutch Birding, 25,* 17-31.

Panov, E. N., Rubtsov, A. S., & Mordkovich, M. V. (2007). New data on the relationships between two species of buntings (*Emberiza citrinella* and *E. leucocephalos*) hybridizing in the areas of overlap of their ranges, *Zoologicheskii Zhurnal, 86*(11), 1362–1378.

Paradis, E., & Schliep, K. (2019). ape 5.0: An environment for modern phylogenetics and evolutionary analyses in R. *Bioinformatics, 35*(3), 526-528. doi:10.1093/bioinformatics/bty633

Price, T. (2008). *Speciation in birds*. Roberts and Co.

R Core Team (2014). R: A language and environment for statistical computing. Vienna, Austria: R Foundation for Statistical Computing. Retrieved from http://www.r-project.org/

832 Rubtsov, A.S. 2007. Variability of songs of the yellowhammer (*Emberiza citrinella*) and pine
833 bunting (*Emberiza leucocephala*) as an evidence of population structure and evolutionary
834 history of the species, *Zoologicheskii Zhurnal, 86*(7), 863–876.

835

836 Rubtsov, A. S., & Tarasov, V. V. (2017). Relations between the yellowhammer (*Emberiza*
837 *citrinella*) and the pine bunting (*Emberiza leucocephalos*) in the forested steppe of the
838 Trans-Urals. *Biology Bulletin, 44*(9), 1059-1072. doi:10.1134/S1062359017090114

839

840 Ruegg, K., Anderson, E. C., Boone, J., Pouls, J., & Smith, T. B. (2014). A role for migration-
841 linked genes and genomic islands in divergence of a songbird. *Molecular Ecology,*
842 *23*(19), 4757-4769. doi:10.1111/mec.12842

843

844 Sackton, T. B., Corbett-Detig, R. B., Nagaraju, J., Vaishna, L., Arunkumar, K. P., & Hartl, D. L.
845 (2014). Positive selection drives faster-z evolution in silkmoths. *Evolution, 68*(8), 2331-
846 2342. doi:10.1111/evo.12449

847

848 Sackton, T. B., Haney, R. A., & Rand, D. M. (2003). Cytonuclear coadaptation in *Drosophila*:
849 Disruption of cytochrome c oxidase activity in backcross genotypes. *Evolution, 57*(10),
850 2315-2325. https://doi.org/10.1111/j.0014-3820.2003.tb00243.x

851

852 Saraste, M. (1999). Oxidative phosphorylation at the fin de siècle. *Science, 283*(5407), 1488-
853 1493. https://doi.org/10.1126/science.283.5407.1488

854

855 Scordato, E. S. C., Wilkins, M. R., Semenov, G., Rubtsov, A. S., Kane, N. C., & Safran, R. J.
856 (2017). Genomic variation across two barn swallow hybrid zones reveals traits associated
857 with divergence in sympatry and allopatry. *Molecular Ecology, 26*(20), 5676-
858 5691. https://doi.org/10.1111/mec.14276

859

860 Sloan, D. B., Havird, J. C., & Sharbrough, J. (2017). The on-again, off-again relationship
861 between mitochondrial genomes and species boundaries. *Molecular Ecology, 26*(8),
862 2212-2236. doi:10.1111/mec.13959

863

864 Smukowski, C. S., & Noor, M. A. F. (2011). Recombination rate variation in closely related
865 species. *Heredity, 107*(6), 496-508. doi:10.1038/hdy.2011.44

866

867 Stacklies, W., Redestig, H., Scholz, M., Walther, D., & Selbig, J. (2007). pcaMethods-a
868 bioconductor package providing PCA methods for incomplete data. *Bioinformatics,*
869 *23*(9), 1164-1167. doi:10.1093/bioinformatics/btm069

870

871 Tajima, F. (1989). Statistical method for testing the neutral mutation hypothesis by DNA
872 polymorphism. *Genetics, 123*(3), 585-595.

873

874 Thornton, K., & Long, M. (2002). Rapid divergence of gene duplicates on the *Drosophila*
875 *melanogaster* X chromosome. *Molecular Biology and Evolution, 19*(6), 918-925.
876 doi:10.1093/oxfordjournals.molbev.a004149

877

878 Toews, D. P. L., & Brelsford, A. (2012). The biogeography of mitochondrial and nuclear
879 discordance in animals. *Molecular Ecology, 21*(16), 3907-3930. doi:10.1111/j.1365-
880 294X.2012.05664.x

881

882 Turner, S. (2018). qqman: An R package for visualizing GWAS results using Q-Q and
883 Manhattan plots. *Journal of Open Source Software, 3*(25), 731. doi:10.21105/joss.00731

884

885 Wang, S., Ore, M. J., Mikkelsen, E. K., Lee-Yaw, J., Toews, D. P. L., Rohwer, S., & Irwin, D.
886 (2021). Signatures of mitonuclear coevolution in a warbler species complex. *Nature*
887 *Communications*, in press. doi:10.1038/s41467-021-24586-8

888

889 Warren, W. C., Clayton, D. F., Ellegren, H., Arnold, A. P., Hillier, L. W.,Künstner, A., Searle,
890 S., White, S., Vilella, A. J., Fairley, S., Heger, A., Kong, L., Ponting, C. P., Jarvis, E. D.,
891 Mello, C. V., Minx, P., Lovell, P., Velho, T. A. F., Ferris, M., … Wilson, R. K. (2010).
892 The genome of a songbird. *Nature, 464*(7289), 757–762. doi:10.1038/nature08819

893

894 Weir, B. S., & Cockerham, C. C. (1984). Estimating F-statistics for the analysis of population
895 structure. *Evolution, 38*(6), 1358-1370. doi:10.1111/j.1558-5646.1984.tb05657.x

896

897 Wu, C. (2001). The genic view of the process of speciation. *Journal of Evolutionary*
898 *Biology, 14*(6), 851-865. doi:10.1046/j.1420-9101.2001.00335.x

899

900 Yannic, G., Dubey, S., Hausser, J., & Basset, P. (2010). Additional data for nuclear DNA give
901 new insights into the phylogenetic position of *Sorex granarius* within the *Sorex araneus*

902 group. *Molecular Phylogenetics and Evolution, 57*(3), 1062-
903 1071. https://doi.org/10.1016/j.ympev.2010.09.015

904

905 Zink, R. M., & Barrowclough, G. F. (2008). Mitochondrial DNA under siege in avian
906 phylogeography. *Molecular Ecology, 17*(9), 2107-2121. doi:10.1111/j.1365-
907 294X.2008.03

Tables

Table 1. Geographical locations and sample sizes of the sites included in this study. Sampling locations may include multiple sites that appeared too close together to be shown in detail in Figure 1A. Full details for the sites included in each sampling locations can be found in Supplementary Table 1. The sampling location numbers that appear in the "Sampling Location" column correspond to those that appear in red in Figure 1A. The "Sample Size" columns describes the total number of samples collected from a particular location.

Sampling Location	Latitude (°N)	Longitude (°E)	*E. citrinella* sample size	*E. leucocephalos* sample size
1	57.99	12.49	1	0
2	59.81	17.05	1	0
3	51.71	18.61	1	0
4	55.28	20.97	5	0
5	65.86	21.48	2	0
6	51.38	35.84	3	0
7	55.97	38.50	18	0
8	61.45	38.67	12	0
9	43.54	40.47	1	0
10	65.85	44.24	1	0
11	58.33	44.76	1	0
12	51.20	57.27	7	0
13	49.64	110.17	0	2
14	50.66	115.09	0	17
15	51.12	118.56	0	15
16	50.56	143.08	0	8
		Total	**53**	**42**

Table 2. Summary statistics calculated while conducting mitonuclear co-introgression analysis. A total of 7187 windows, each of 2000 bp of obtained sequence, were considered when determining introgression windows. A total of 134 mitonuclear genes were investigated for signals of co-introgression. "*" indicates a significant p-value.

Species	# of introgression windows identified	% of mitonuclear genes appearing in introgression windows	Binomial test p-value	Fisher's Exact test p-value
Yellowhammer	244	6.7	0.04952*	0.1311
Pine bunting	222	3.0	1	1

Table 3. Identities, chromosomal locations, windowed Tajima's D values and functions of mitonuclear genes that appeared within 244 yellowhammer introgression windows. In the "Mitonuclear Gene Function" column, ETC stands for "Electron Transport Chain". Mitonuclear gene names are written as they appear in Hill (2019).

Mitonuclear Gene	Chromosome where mitonuclear gene is found	Windowed Tajima's D Value	Mitonuclear Gene Function
APOPT1	5	-2.207	Assembly factor/ancillary protein for ETC complex IV
COX5A	10	-2.420	Structural subunit of ETC complex IV
COX17	1	-2.509	Assembly factor/ancillary protein for ETC complex IV
MRPL1	4	-2.207	Mitochondrial large ribosomal subunit protein
MRPL27	18	-2.214	Mitochondrial large ribosomal subunit protein
MRPL32	2	-2.306	Mitochondrial large ribosomal subunit protein
NDUFC1	4	-2.399	Structural subunit of ETC complex I
mtSSB	1A	-2.362	Single stranded DNA-binding protein
UQCR11	28	-2.499	Structural subunit of ETC complex III

Table 4. Identities, chromosomal locations, windowed Tajima's D values and functions of mitonuclear genes that appeared within 222 pine bunting introgression windows. In the "Mitonuclear Gene Function" column, ETC stands for "Electron Transport Chain". Mitonuclear gene names are written as they appear in Hill (2019).

Mitonuclear Gene	Chromosome where mitonuclear gene is found	Windowed Tajima's D Value	Mitonuclear Gene Function
ATP5H5I	18	-2.601	Structural subunit of ETC complex V
COX5A	10	-2.545	Structural subunit of ETC complex IV
MRPL2	3	-2.247	Mitochondrial large ribosomal subunit protein
NDUFB4	1	-2.304	Structural subunit of ETC complex I

Figures

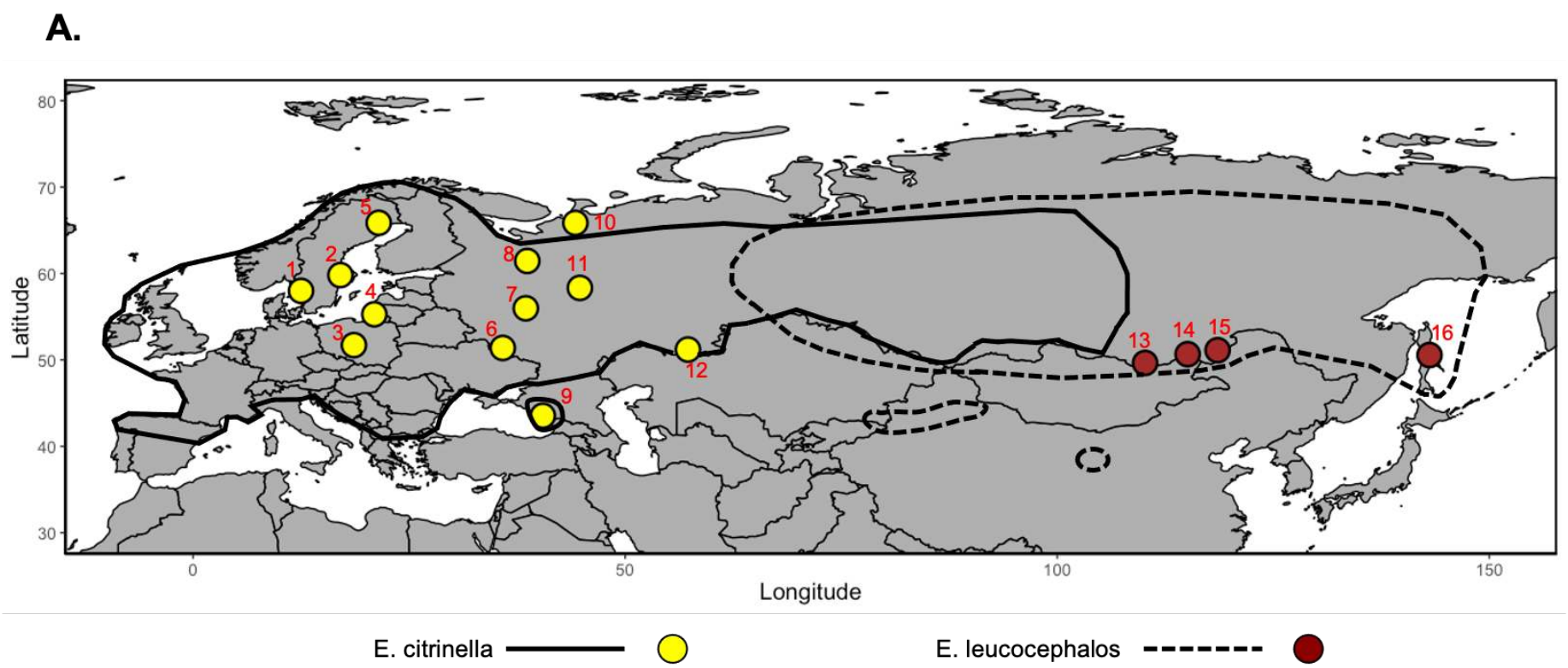
A.
Latitude
Longitude
80
70
60
50
40
30
0
50
100
150
1
2
3
4
5
6
7
8
9
10
11
12
13
14
15
16
E. citrinella
E. leucocephalos
B.
Emberiza citrinella
Emberiza leucocephalos
Pure Citrinella (PC)
Almost Citrinella (SC)
Pure Leucocephalos (PL)
Almost Leucocephalos (SL)

Figure 1. A) Map of sampling locations included in this study. Red numbers accompanying each location correspond to the sampling location numbers appearing in Table 1 which also describes sample sizes. Sampling locations may include multiple sites that appeared too close together to be shown in detail in this figure. Full details for the sites included in each sampling location can be found in Supplementary Table 1. Sampling location points are coloured based on the taxon caught in each area: yellowhammer (*Emberiza citrinella*; yellow) and pine bunting (*Emberiza leucocephalos*; brown). The solid black line indicates the geographic range of the yellowhammer and the dashed black line indicates the geographic range of the pine bunting as described in Irwin et al. (2009). **B)** Photos of plumage variation between yellowhammers and pine buntings. Each photo represents one of four phenotypic classes: PC, SC, PL and SL. Individuals with a PC and SC phenotypic class were grouped together as *Emberiza citrinella* and individuals with a PL and SL phenotypic class were grouped together as *Emberiza leucocephalos*. All photos are credited to Dr. Alexander Rubtsov.

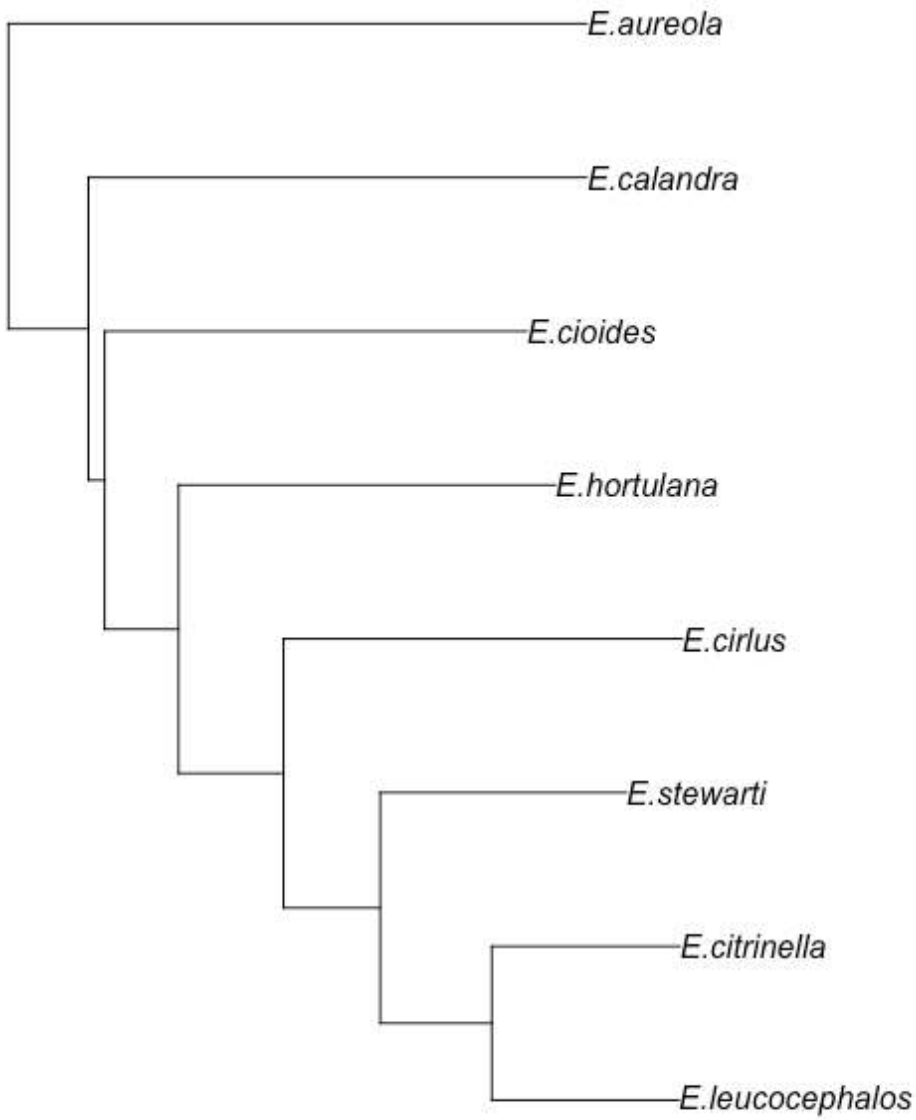

Figure 2. Unrooted neighbour-joining tree of Emberizidae species constructed based on average absolute between-population nucleotide diversity (π_B). Sample sizes for each species are as follows: *E. aureola* = 1, *E. calandra* = 1, *E. cioides* = 1, *E. hortulana* = 1, *E. cirlus* = 6, *E. stewarti* = 4, *E. citrinella* = 53 and *E. leucocephalos* = 42.

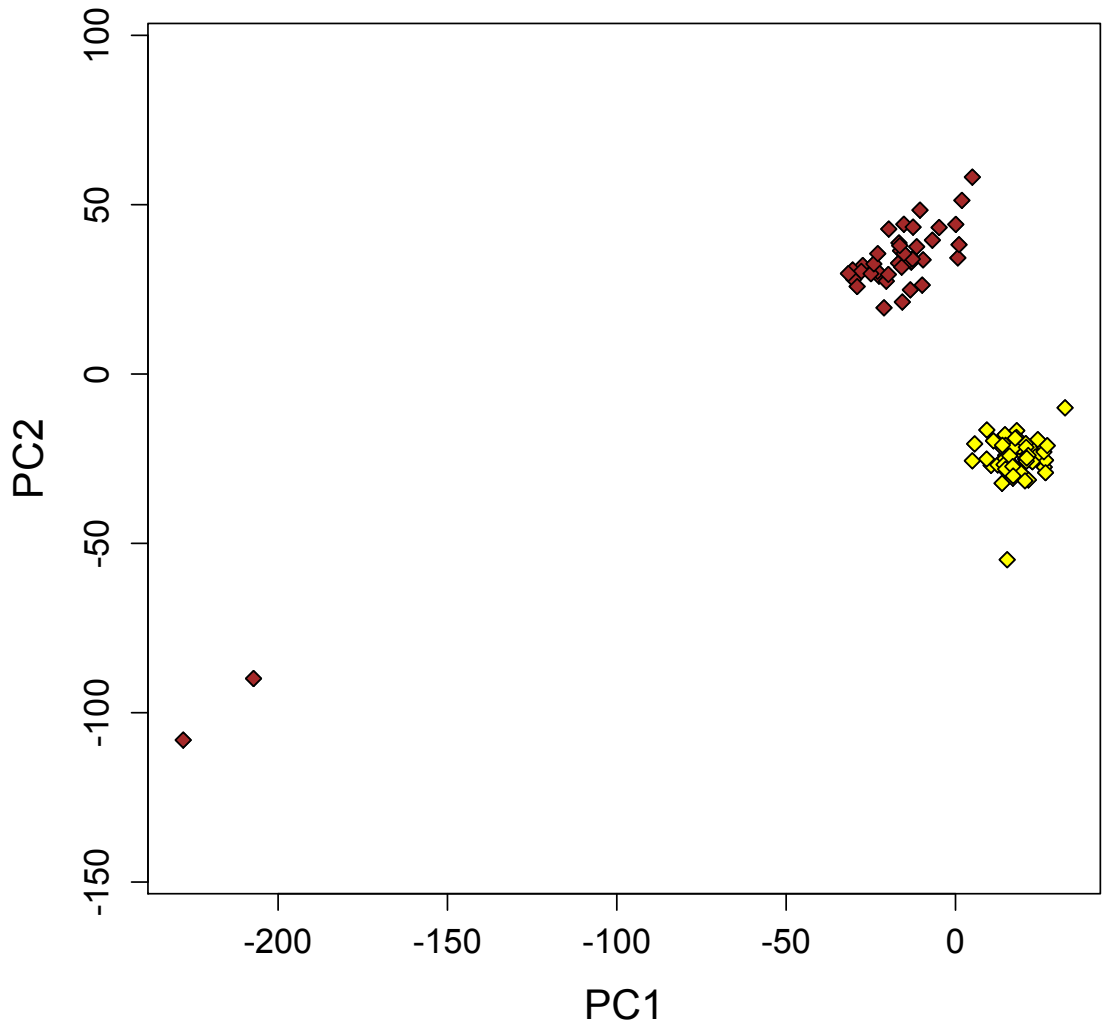

Figure 3. PCA of genetic variation between allopatric yellowhammers (yellow; n = 53) and allopatric pine buntings (brown; n = 42), based on 374,780 genome-wide SNPs. PC1 and PC2 explain 3.6% and 2.9%, respectively, of the variation among individuals.

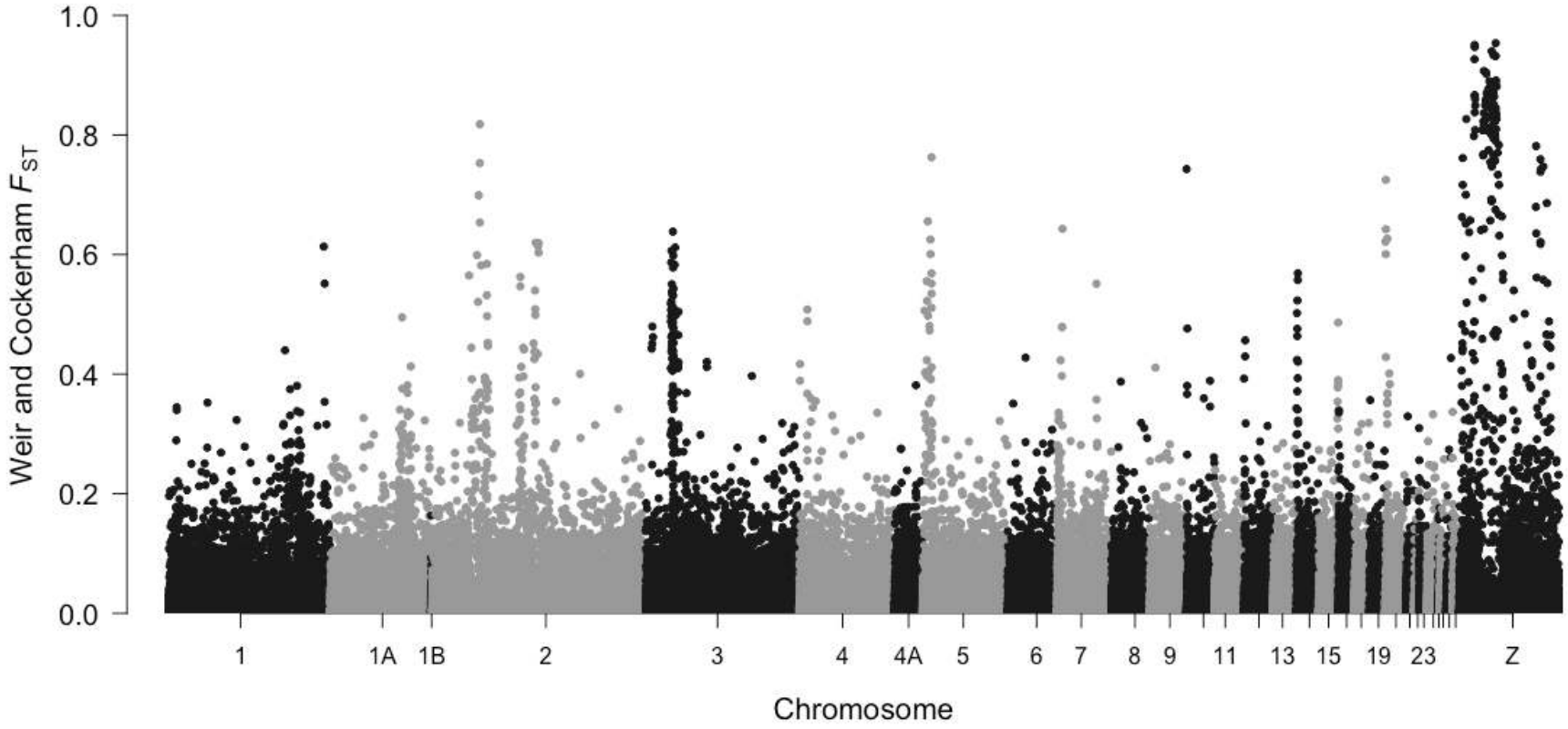

Figure 4. Relative differentiation (F_{ST}) of 349,807 genome-wide SNPs identified between allopatric yellowhammers (n = 53) and allopatric pine buntings (n = 42), with chromosomes represented with alternating black and grey. Narrow regions of elevated differentiation can be seen on many autosomes, and there are broad regions of high differentiation on the Z chromosome.

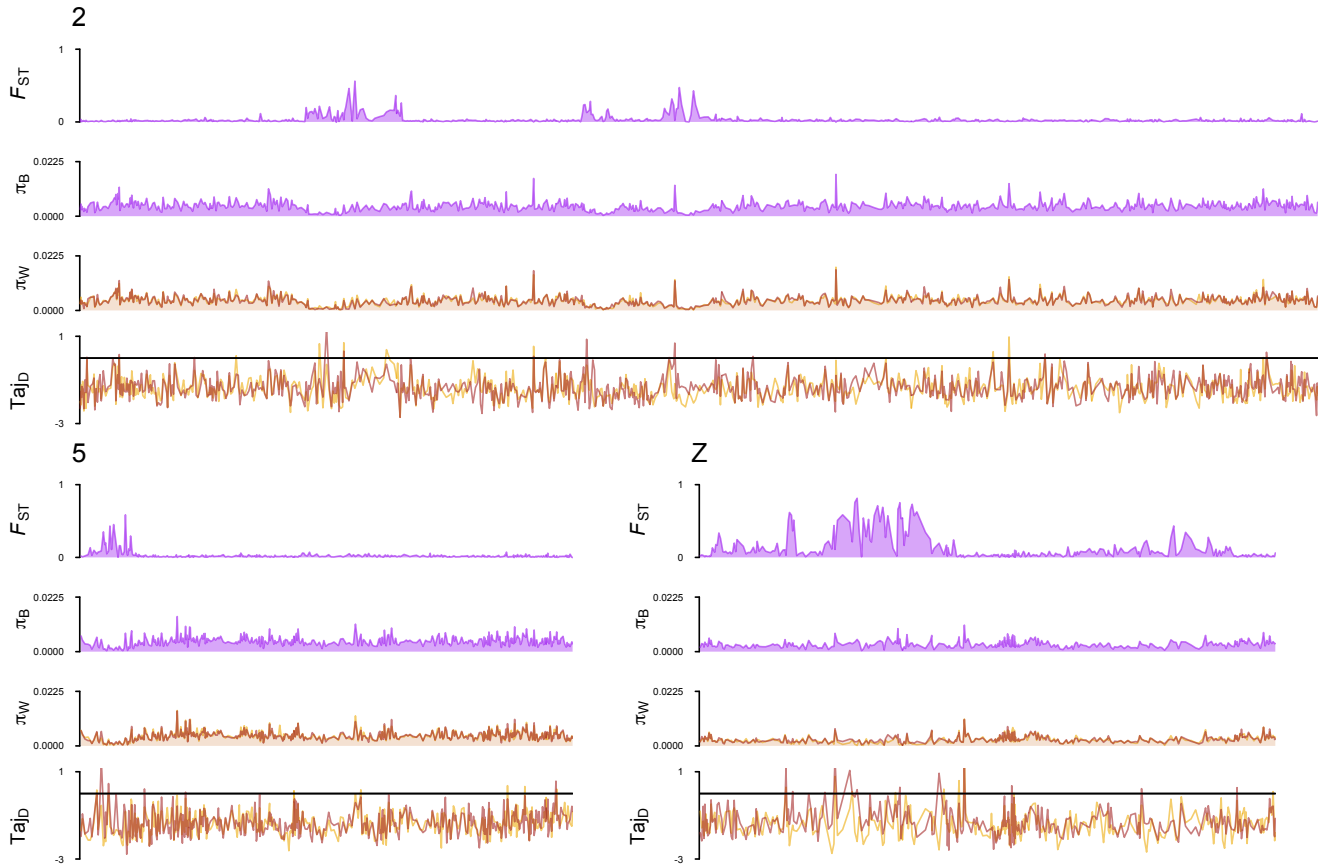

Figure 5. Patterns of genetic variation comparing allopatric yellowhammers (n = 53) and allopatric pine buntings (n = 42) across three chromosomes (2, 5 and Z). Relative nucleotide differentiation (F_{ST}), absolute between-population nucleotide diversity (π_B), absolute within-population nucleotide diversity (π_W) and Tajima's D (Taj_D) are shown as 2000 bp windowed averages across each chromosome. F_{ST} and π_B are shown as purple lines to indicate that values were calculated as a comparison between allopatric yellowhammers and pine buntings. π_W and Taj_D are shown as two separate lines (yellow = yellowhammers, brown = pine buntings) to indicate that values were calculated separately for each population.

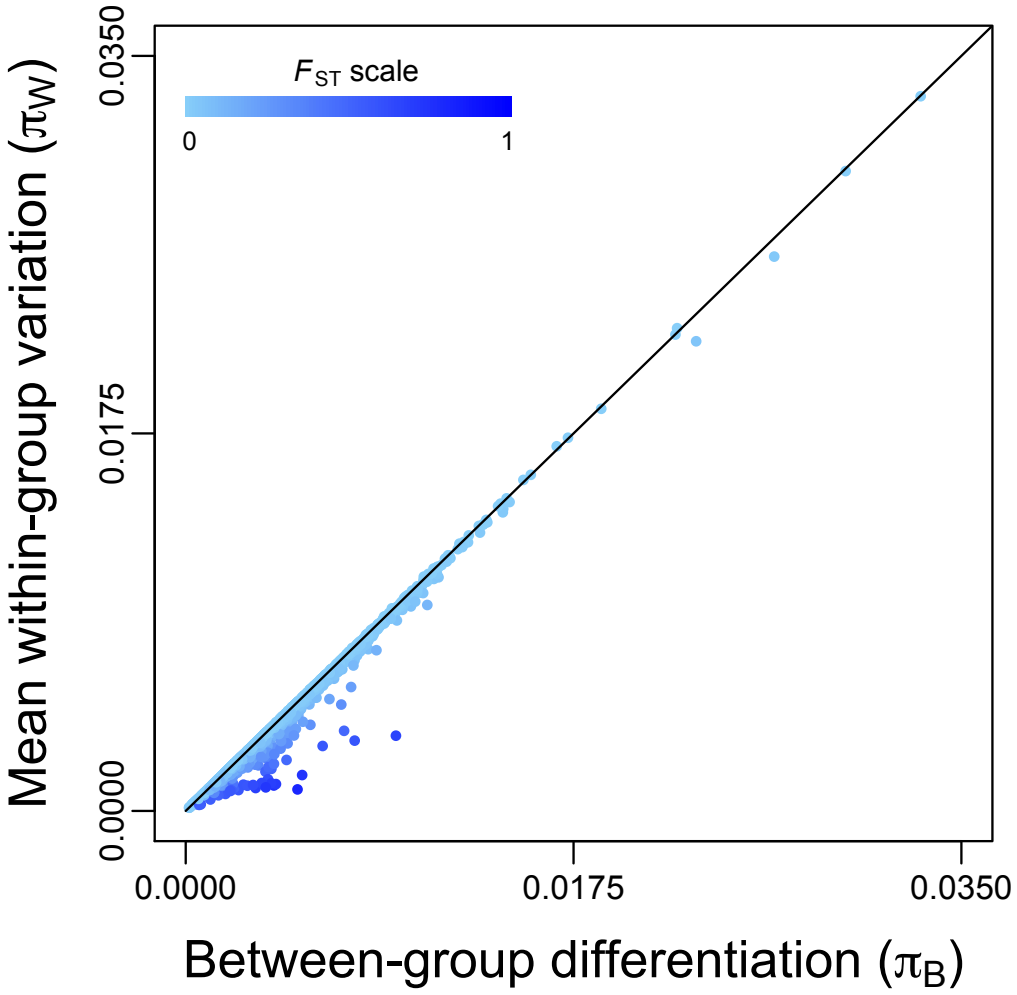

Figure 6. Mean absolute within-group nucleotide diversity (π_W) of allopatric yellowhammers (n = 53) and allopatric pine buntings (n =42) plotted against absolute between-group nucleotide diversity (π_B). Each dot represents the average value taken from a 2000 bp window of sequenced data across the nuclear genome. The black line indicates where mean within-group nucleotide diversity equals between-group nucleotide diversity. Increasing values of relative differentiation (F_{ST}) calculated for each window are shown in darker shades of blue.

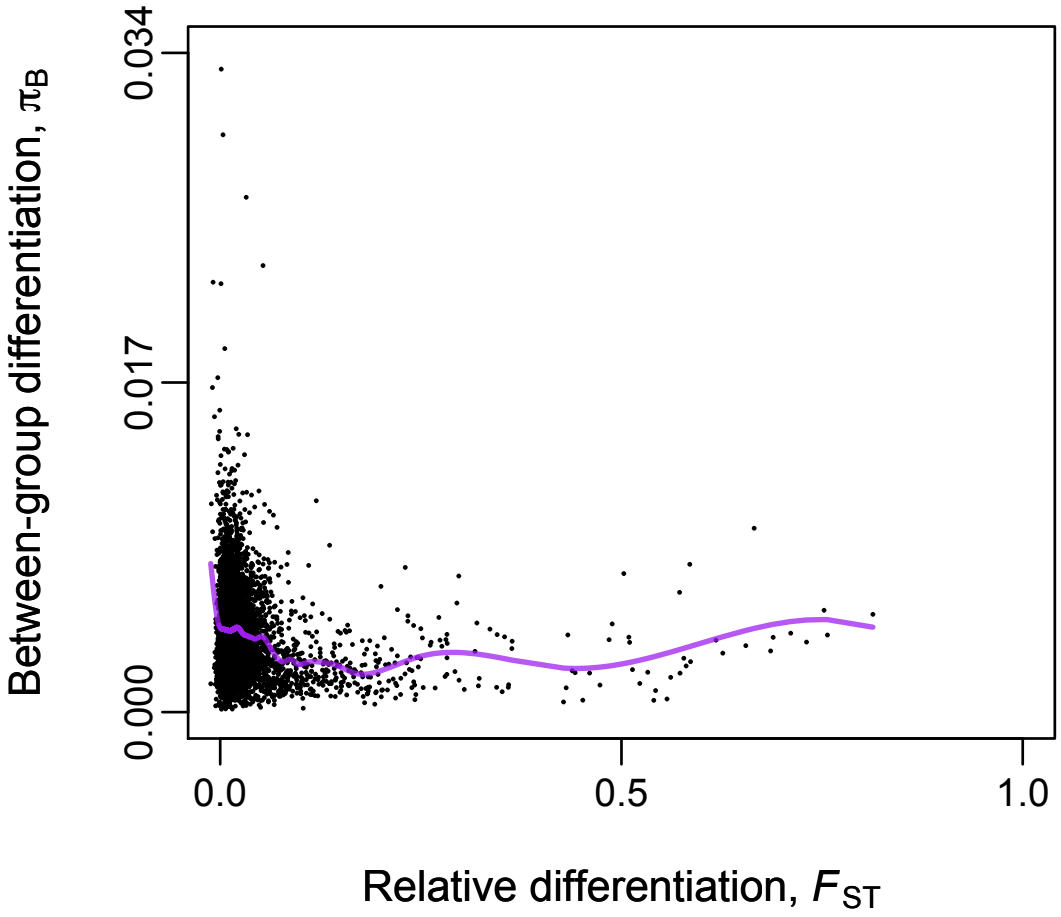

Figure 7. Association between relative differentiation (F_{ST}) and absolute between-group nucleotide diversity (π_B) of allopatric yellowhammers (n=53) and allopatric pine buntings (n = 42). Each black dot represents average values calculated from a 2000 bp window of sequenced data. A cubic spline fit between the variables is shown as a purple line.